

## Supplementary Materials

### Systematic Assessment of Adsorption-Coupled Electron Transfer toward Voltammetric Discrimination of Concerted and Non-Concerted Mechanisms

Donald C. Janda,<sup>a</sup> Kiran Barma,<sup>a,b</sup> Niraja Kurapati,<sup>a</sup> Oleksiy V. Klymenko,<sup>c,d</sup> Alexander Oleinick,<sup>c</sup> Irina Svir,<sup>c,e</sup> Christian Amatore,<sup>c,f</sup> and Shigeru Amemiya<sup>a,\*</sup>

<sup>a</sup> Department of Chemistry, University of Pittsburgh, 219 Parkman Avenue, Pittsburgh, Pennsylvania, 15260, United States

<sup>b</sup> UM-DAE, Center for Excellence in Basic Sciences, University of Mumbai, Mumbai, 400098, India

<sup>c</sup> PASTEUR, Département de chimie, École normale supérieure, PSL Université, Sorbonne Université, CNRS, 75005 Paris, France

<sup>d</sup> Present address: Department of Chemical and Process Engineering, University of Surrey, Guildford GU2 7XH, United Kingdom

<sup>e</sup> Design Automation Department, Kharkiv National University of Radio Electronics, Nauky Avenue, 14, Kharkiv 61166, Ukraine

<sup>f</sup> State Key Laboratory of Physical Chemistry of Solid Surfaces, College of Chemistry and Chemical Engineering, Xiamen University, Xiamen, 361005, China

\* To whom correspondence should be addressed. E-mail: amemiya@pitt.edu. Fax: 412-624-8611.

## Table of Contents

Symbol	3
Dimensionless Model	5
Kinetic Zone Diagram	10
ET Equivalence	16
Quantitative Discrimination between Similar CVs	18
Adsorption-Coupled Reduction of Benzyl Chloride	19
References	26

**Table S-1. List of Symbols Used in This Work.**

Symbol	Meaning <sup>a,b</sup>	Definition	Dimensionless	
			Symbol	Definition
$c_i$	concentration of species i in the solution	eq 10	$C_i$	eq S-1
$\Gamma_i$	surface concentration of species i	eq 11	$\theta_i$	eq S-5
$\Gamma_M$	surface concentration of free adsorption site	eq 11	$\theta_M$	eq S-5
$\Gamma_s$	total surface concentration of adsorption site	eq 9	$\kappa$	eq 17
$v_{ads}^i$	rate for adsorption of species i	eq 11	$V_{ads}^i$	eq S-5
$k_{ads}^i$	rate constant for adsorption of species i	eq 11	—	—
$k_{des}^i$	rate constant for desorption of species i	eq 11	$\lambda_{des}^i$	eq 18
$\beta_i$	equilibrium constant for adsorption of species i	eq 12	$\rho_i$	eq 19
$E$	electrode potential	eq 13	— <sup>c</sup>	—
$\alpha$	transfer coefficient	eq 13	—	—
$v_C^j$	adsorption-coupled reduction rate for species j	eq 13	$V_C^j$	eq S-11
$k_{red}^j$	rate constant for reduction of species j	eq 13	—	—
$k_{ox}^j$	rate constant for oxidation of species j	eq 13	—	—
$E_{app}^j$	apparent formal potential for ACET of species j	eq 13	—	—
$k_C^{0,j}$	standard rate constant for ACET of species j	eq S-8	$\Lambda_C^j$	eq S-11
$E_C^{0',j}$	formal potential for ACET of species j	eq S-8	$\xi_C^j$	eq S-11
$v_{IS}^O$	rate of inner-sphere reduction	eq 15	$V_{IS}^O$	eq S-16

$k_{IS}^{0,O_{ads}}$	standard rate constant of inner-sphere ET reaction	eq 15	$\Lambda_{IS}^{O_{ads}}$	eq S-16
$E_{IS}^{0,O_{ads}}$	formal potential of inner-sphere ET reaction	eq 15	$\xi_{IS}^{O_{ads}}$	eq S-16
$v_{OS}^O$	rate of outer-sphere reduction	eq 16	$V_{OS}^O$	eq S-17
$k_{OS}^{0,O}$	standard rate constant of outer-sphere ET reaction	eq 16	$\Lambda_{OS}^O$	eq S-17
$E_{OS}^{0,O}$	formal potential of outer-sphere ET reaction	eq 16	$\xi_{OS}^O$	eq S-17
$i_{et}$	current	eq 7	$I$	eq 9
$A$	electrode area	eq 7	—	—
$v$	potential scan rate	eq 9	—	—
$D$	diffusion coefficient	eq 10	—	—
$x$	distance from the electrode surface	eq 10	$X$	eq S-4
$t$	time	eq 10	$\tau$	eq S-3
$k_{prot}^C$	rate constant for protonation of species C	eq S-18	$K_{prot}^C$	eq S-22
$v_{prot}^{C_{ads}}$	rate for protonation of species $C_{ads}$	eq S-23	$V_{prot}^{C_{ads}}$	eq S-24
$k_{prot}^{C_{ads}}$	rate constant for protonation of species $C_{ads}$	eq S-23	$K_{prot}^{C_{ads}}$	eq S-25
$i_{diff}^p$	diffusion-limited peak current	Table S-4	$I_{diff}^p$	Table S-6
$i_{ET}^p$	current for reversible ET of saturated adsorbate	Table S-4	$I_{ET}^p$	Table S-6
$i_{ET,i_{ads}}^p$	current for reversible ET of unsaturated adsorbate	Table S-4	$I_{ET,O_{ads}}^p$	Table S-6
$i_{R_{sat}}^{lim}$	limiting current for desorption of saturated adsorbate	Table S-5	$I_{R_{sat}}^{lim}$	Table S-7
$i_{R_{sat}}^{pc}$	peak current for saturated adsorption	Table S-5	$I_{R_{ads}}^{pc}$	Table S-7
$i_{R_{sat}}^{pa}$	peak current for desorption of saturated adsorption	Table S-5	$I_{R_{sat}}^{pa}$	Table S-7

$i_{i_{\text{ads}}}^{\text{lim}}$	limiting current for saturated adsorption	Table S-5	$I_{O_{\text{ads}}}^{\text{lim}}$	Table S-6
$i_{R_{\text{ads}}}^{\text{p}}$	peak current for desorption of unsaturated adsorbate	Table S-5	$I_{R_{\text{ads}}}^{\text{p}}$	Table S-7

<sup>a</sup>  $i = \text{R or O}$ . <sup>b</sup>  $j = \text{O or O}_{\text{ads}}$ . <sup>c</sup> See definitions of formal potentials.

**Dimensionless Model.** Cyclic voltammograms (CVs) of concerted and non-concerted mechanisms were simulated in the dimensionless form by employing COMSOL Multiphysics 5.6 (COMSOL, Burlington, MA). The normalised current (eq 9) was simulated for the cycle of the potential at the scan rate of  $v$ . A diffusion equation for species,  $i$  ( $= \text{O or R}$ ), is given in either mechanism by eq 10 and solved in the dimensionless form given by

$$\frac{\partial C_i}{\partial \tau} = \left( \frac{\partial^2 C_i}{\partial X^2} \right) \quad (\text{S-1})$$

with

$$C_i = \frac{c_i}{c_0} \quad (\text{S-2})$$

$$\tau = \frac{Fv t}{RT} \quad (\text{S-3})$$

$$X = x \sqrt{\frac{Fv}{RTD}} \quad (\text{S-4})$$

The adsorption rate of species  $i$  is given by eq 11 and is normalised to yield

$$V_{\text{ads}}^i = v_{\text{ads}}^i \frac{RT}{\Gamma_s Fv} = \lambda_{\text{des}}^i \left\{ \rho_i C_i \theta_M - \theta_i \right\} \quad (\text{S-5})$$

with

$$\theta_i = \frac{\Gamma_i}{\Gamma_s} \quad (\text{S-6})$$

At the equilibrium, eq S-5 with  $V_{\text{ads}}^i = 0$  is equivalent to the Langmuir isotherm as given by

$$\rho_i C_i = \frac{\theta_i}{\theta_M} \quad (\text{S-7})$$

The rates of ET steps are defined by eqs 13–16 and normalised with dimensionless parameters (Table S-2). The rate of the ACET step given by eq 13 is rearranged to yield

$$v_C^{\text{O}} = k_C^{\text{O},\text{O}} \left\{ C_{\text{O}} \theta_{\text{M}} \exp \left[ -\frac{\alpha F}{RT} (E - E_C^{\text{O},\text{O}}) \right] - \theta_{\text{R}} \exp \left[ \frac{(1-\alpha) F}{RT} (E - E_C^{\text{O},\text{O}}) \right] \right\} \quad (\text{S-8})$$

with

$$k_C^{\text{O},\text{O}} = \left( k_{\text{red}}^{\text{O}} c_0 \right)^{1-\alpha} \left( k_{\text{ox}}^{\text{O}} \right)^{\alpha} \Gamma_{\text{s}} \quad (\text{S-9})$$

$$E_C^{\text{O},\text{O}} = E_{\text{app}}^{\text{O}} + \frac{RT}{F} \ln \frac{k_{\text{red}}^{\text{O}} c_0}{k_{\text{ox}}^{\text{O}}} \quad (\text{S-10})$$

where  $k_C^{\text{O},\text{O}}$  and  $E_C^{\text{O},\text{O}}$  correspond to rate constant and formal potential, respectively, at the standard state, i.e.,  $c_{\text{O}} = c_0 = 1 \text{ M}$  and  $\theta_{\text{M}} = \theta_{\text{R}} = 0.5$ . Eq S-8 is normalised to define the dimensionless rate of the ACET step as

$$V_C^{\text{O}} = v_C^{\text{O}} \frac{RT}{\Gamma_{\text{s}} F v} = \Lambda_C^{\text{O}} \left[ C_{\text{O}} \theta_{\text{M}} \left( \xi_C^{\text{O}} \right)^{-\alpha} - \theta_{\text{R}} \left( \xi_C^{\text{O}} \right)^{(1-\alpha)} \right] \quad (\text{S-11})$$

Similarly, eq 14 for the rate of the ACET step is rearranged to yield

$$v_C^{\text{O}_{\text{ads}}} = k_C^{\text{O}_{\text{ads}},\text{O}_{\text{ads}}} \left\{ \theta_{\text{O}} \exp \left[ -\frac{\alpha F}{RT} (E - E_C^{\text{O}_{\text{ads}},\text{O}_{\text{ads}}}) \right] - C_{\text{R}} \theta_{\text{M}} \exp \left[ \frac{(1-\alpha) F}{RT} (E - E_C^{\text{O}_{\text{ads}},\text{O}_{\text{ads}}}) \right] \right\} \quad (\text{S-12})$$

with

$$k_C^{\text{O}_{\text{ads}},\text{O}_{\text{ads}}} = \left( k_{\text{red}}^{\text{O}_{\text{ads}}} \right)^{1-\alpha} \left( k_{\text{ox}}^{\text{O}_{\text{ads}}} c_0 \right)^{\alpha} \Gamma_{\text{s}} \quad (\text{S-13})$$

$$E_C^{\text{O}_{\text{ads}},\text{O}_{\text{ads}}} = E_{\text{app}}^{\text{O}_{\text{ads}}} + \frac{RT}{F} \ln \frac{k_{\text{red}}^{\text{O}_{\text{ads}}} c_0}{k_{\text{ox}}^{\text{O}_{\text{ads}}}} \quad (\text{S-14})$$

where  $k_C^{0, O_{\text{ads}}}$  and  $E_C^{0', O_{\text{ads}}}$  are equivalent to rate constant and formal potential at the standard state with

$c_R = c_0 = 1 \text{ M}$  and  $\theta_M = \theta_O = 0.5$ . Eq S-12 can be normalised to yield the dimensionless ACET rate as

$$V_C^{\text{O}_{\text{ads}}} = v_C^{\text{O}_{\text{ads}}} \frac{RT}{\Gamma_s F \nu} = \Lambda_C^{\text{O}_{\text{ads}}} \left[ \theta_O \left( \xi_C^{\text{O}_{\text{ads}}} \right)^{-\alpha} - C_R \theta_M \left( \xi_C^{\text{O}_{\text{ads}}} \right)^{(1-\alpha)} \right] \quad (\text{S-15})$$

In addition, the dimensionless rates of inner-sphere and outer-sphere ET steps are obtained from eqs 15 and 16, respectively, as

$$V_{\text{IS}}^{\text{O}_{\text{ads}}} = v_{\text{IS}}^{\text{O}_{\text{ads}}} \frac{RT}{\Gamma_s F \nu} = \Lambda_{\text{IS}}^{\text{O}_{\text{ads}}} \left[ \theta_O \left( \xi_{\text{IS}}^{\text{O}_{\text{ads}}} \right)^{-\alpha} - \theta_R \left( \xi_{\text{IS}}^{\text{O}_{\text{ads}}} \right)^{(1-\alpha)} \right] \quad (\text{S-16})$$

$$V_{\text{OS}}^{\text{O}} = \frac{v_{\text{OS}}^{\text{O}}}{c_0} \sqrt{\frac{RT}{F \nu D}} = \Lambda_{\text{OS}}^{\text{O}} \left[ C_O \left( \xi_{\text{OS}}^{\text{O}} \right)^{-\alpha} - C_R \left( \xi_{\text{OS}}^{\text{O}} \right)^{(1-\alpha)} \right] \quad (\text{S-17})$$

Eq S-1 is solved with dimensionless boundary conditions (Table S-3) to obtain a normalised current response,  $I$ , against the electrode potential. In Case II, the surface concentration of adsorption sites is given by  $\Gamma_M = \Gamma_s - \Gamma_O - \Gamma_R$ . The corresponding concerted mechanism involves an ACET step to yield  $I = V_C^{\text{O}}$ . Alternatively, the non-concerted mechanism is based on an inner-sphere ET step to yield  $I = V_{\text{IS}}^{\text{O}_{\text{ads}}}$ . In Case III, the surface concentration of adsorption sites is given by  $\Gamma_M = \Gamma_s - \Gamma_R$ . The normalised current in the concerted mechanism is given by  $I = V_C^{\text{O}}$ . In the non-concerted mechanism, the normalised current is given by  $I = V_{\text{OS}}^{\text{O}} / \kappa$ . The simulation of Case IV is detailed later.

**Table S-2. Dimensionless Parameters and Nernst Equations for ET Steps**

ET Rate	Standard ET Rate Constant	Electrode Potential	Nernst Equation
$V_{OS}^O$	$\Lambda_{OS}^O = k_{OS}^{0,O} \sqrt{\frac{RT}{FvD}}$	$\xi_{OS}^O = \exp\left[\frac{F}{RT}(E - E_{OS}^{0',O})\right]$	$\xi_{OS}^O = \frac{C_O}{C_R}$
$V_{IS}^{O_{ads}}$	$\Lambda_{IS}^{O_{ads}} = k_{IS}^{0,O_{ads}} \frac{RT}{Fv}$	$\xi_{IS}^{O_{ads}} = \exp\left[\frac{F}{RT}(E - E_{IS}^{0',O_{ads}})\right]$	$\xi_{IS}^{O_{ads}} = \frac{\theta_O}{\theta_R}$
$V_C^O$	$\Lambda_C^O = k_C^{0,O} \frac{RT}{\Gamma_s Fv}$	$\xi_C^O = \exp\left[\frac{F}{RT}(E - E_C^{0',O})\right]$	$\xi_C^O = \frac{C_O \theta_M}{\theta_R}$
$V_C^{O_{ads}}$	$\Lambda_C^{O_{ads}} = k_C^{0,O_{ads}} \frac{RT}{\Gamma_s Fv}$	$\xi_C^{O_{ads}} = \exp\left[\frac{F}{RT}(E - E_C^{0',O_{ads}})\right]$	$\xi_C^{O_{ads}} = \frac{\theta_O}{C_R \theta_M}$



**Table S-3. Electrode Surface Boundary Conditions of Concerted and Non-Concerted Mechanisms in Case II and III**

	Concerted Mechanism		Non-Concerted Mechanism	
Case II	Original Condition	Dimensionless Condition	Original Condition	Dimensionless Condition
O	$-D \left( \frac{\partial c_O}{\partial x} \right) = -v_C^O - v_{\text{ads}}^O$	$-\left( \frac{\partial C_O}{\partial X} \right) = -\kappa (V_C^O + V_{\text{ads}}^O)$	$-D \left( \frac{\partial c_O}{\partial x} \right) = -v_{\text{ads}}^O$	$-\left( \frac{\partial C_O}{\partial X} \right) = -\kappa V_{\text{ads}}^O$
O <sub>ads</sub>	$\left( \frac{\partial \Gamma_O}{\partial t} \right) = v_{\text{ads}}^O$	$\left( \frac{\partial \theta_O}{\partial \tau} \right) = V_{\text{ads}}^O$	$\left( \frac{\partial \Gamma_O}{\partial t} \right) = v_{\text{ads}}^O - v_{\text{IS}}^O$	$\left( \frac{\partial \theta_O}{\partial \tau} \right) = V_{\text{ads}}^O - V_{\text{IS}}^O$
R <sub>ads</sub>	$\left( \frac{\partial \Gamma_R}{\partial t} \right) = v_C^O$	$\left( \frac{\partial \theta_R}{\partial \tau} \right) = V_C^O$	$\left( \frac{\partial \Gamma_R}{\partial t} \right) = v_{\text{IS}}^O$	$\left( \frac{\partial \theta_R}{\partial \tau} \right) = V_{\text{IS}}^O$
Case III				
O	$-D \left( \frac{\partial c_O}{\partial x} \right) = -v_C^O$	$-\left( \frac{\partial C_O}{\partial X} \right) = -\kappa V_C^O$	$-D \left( \frac{\partial c_O}{\partial x} \right) = -v_{\text{OS}}^O$	$-\left( \frac{\partial C_O}{\partial X} \right) = -V_{\text{OS}}^O$
R	$-D \left( \frac{\partial c_R}{\partial x} \right) = -v_{\text{ads}}^R$	$-\left( \frac{\partial C_R}{\partial X} \right) = -\kappa V_{\text{ads}}^R$	$-D \left( \frac{\partial c_R}{\partial x} \right) = v_{\text{OS}}^O - v_{\text{ads}}^R$	$-\left( \frac{\partial C_R}{\partial X} \right) = V_{\text{OS}}^O - \kappa V_{\text{ads}}^R$
R <sub>ads</sub>	$\left( \frac{\partial \Gamma_R}{\partial t} \right) = v_C^O + v_{\text{ads}}^R$	$\left( \frac{\partial \theta_R}{\partial \tau} \right) = V_C^O + V_{\text{ads}}^R$	$\left( \frac{\partial \Gamma_R}{\partial t} \right) = v_{\text{ads}}^R$	$\left( \frac{\partial \theta_R}{\partial \tau} \right) = V_{\text{ads}}^R$

**Kinetic Zone Diagrams.** We developed kinetic zone diagrams (Figures 1 and 2) by using both numerical and analytical approaches as follows.

**Step 1.** CVs were simulated numerically for various combinations of  $\lambda_{\text{des}}^i$  and  $\kappa$  with a given  $\rho_1$  value to find a characteristic CV for each kinetic zone.

**Step 2.** A peak or limiting current of a characteristic reversible CV was expressed analytically (Tables S-4 and S-5). The analytical expression was confirmed by the corresponding current of a simulated CV with an electrochemically reversible ET step.

**Step 3.** The boundary between two kinetic zones was defined by using the analytical expressions of their characteristic peak or limiting currents. The resultant analytical expression of each boundary is given in Table S-6 for Case II and Table S-7 for Case III.

In Step 2, characteristic currents are controlled by the ET (Table S-4) or adsorption (Table S-5) steps. The characteristic current based on a reversible ET step can be controlled by a diffusing species (entry 1 in Table S-4) or an adsorbate. In the latter case, different expressions are obtained to represent peak currents when the surface concentration of the adsorbate is saturated, unsaturated and equilibrated, or unsaturated and unknown (i.e.,  $\Gamma_i = \Gamma_s$ ,  $\Gamma_s \beta_{OC0}$ , or  $\Gamma_i$  in entries 2, 3, or 4, respectively). By contrast, the current controlled by the adsorption step (Table S-5) is determined by the adsorption rate (eq 11). The limiting current of the AKinDR/AKinDI zone is controlled by the steady-state desorption of the reductant saturated on the electrode surface through the ACET step (entry 1 in Table S-5). The reductant is also saturated through the non-concerted mechanism in the AIDPR zone to yield a pair of pre-peaks

(entries 2 and 3). The heights of the pre-peaks are related to the adsorption or desorption rate and the surface concentration of an adsorbate, which is half of the saturated concentration. A limiting current is also expected in KinDR/KinDI and KinR'/KinI' zones (entry 4) to yield the same expression. The limiting current is controlled by the steady-state desorption and adsorption of the unsaturated oxidant for concerted and non-concerted mechanisms, respectively, but follows the same expression. The limiting current of the DRAI zone (entry 5) is not observable but is defined as a measure of the steady and irreversible adsorption rate of the unsaturated reductant. The adsorption step competes with the diffusion of the reductant to determine the height of the diffusional peak current during the reverse scan. In the DRKin zone, the desorption of the unsaturated reductant can be nearly equilibrated (entry 4 in Table S-4) or kinetically controlled (entry 6 in Table S-5). In either case, a reverse peak current is obtained when half of the adsorbate is desorbed. The latter also describes the maximum peak current expected for the DRAI zone.

In Step 3, a boundary between kinetic zones is defined mainly when the corresponding characteristic currents are equivalent. The only exception in Case II (Table S-6) is the boundary between KinR and KinR' zones (boundary 6), where the limiting current must be much smaller (i.e., ten times) than the peak current. By contrast, a few exceptions are found in Case III (Table S-7). At boundary 1, DMR and DPR zones are expected when the pre-peak is much smaller (i.e., 100 times) than the diffusional peak). Similarly, boundary 4 compares the pre-peak with the limiting current, which must be substantial (at least 10% of the pre-peak) in the AKinDR zone. Moreover, a transition between DRKin and DRAI zones is defined by boundary 6, where the desorption peak is maximised for both zones but is negligible (i.e., 100 times smaller) for the latter zone. Finally, a transition from the DRAI zone to the DPR zone is defined by boundary 7. A limiting current is defined for the irreversible adsorption of the

reductant in the DRAI zone. In the DPR zone, the limiting current becomes negligible (less than 10%) in comparison with the diffusional current.

**Table S-4. Characteristic Peak Currents Controlled by ET Steps**

Reactant	Kinetic Zone		Current	
	Case II	Case III	Original	Dimensionless
Diffusing Species	DO	DMR, DO, DPR, DRKin, DRAI <sup>a</sup>	$i_{\text{diff}}^{\text{p}} = 0.4463FAc_0\sqrt{\frac{FvD}{RT}}$ <sup>b</sup>	$I_{\text{diff}}^{\text{p}} = \frac{0.4463}{\kappa}$
Saturated Adsorbate	AR	ADMR, AKinDR, AR, ADPR, AIDPR	$i_{\text{ET}}^{\text{p}} = \frac{F^2vA\Gamma_s^c}{4RT}$	$I_{\text{ET}}^{\text{p}} = \frac{1}{4}$
Unsaturated Adsorbate	KinR,	—	$i_{\text{ET}, \text{O}_{\text{ads}}}^{\text{p}} = \frac{F^2vA\Gamma_s\beta_{\text{O}}c_0}{4RT}$	$I_{\text{ET}, \text{O}_{\text{ads}}}^{\text{p}} = \frac{\rho_{\text{O}}}{4}$
	KinR'	—		
	—	DO, DRKin <sup>d</sup>	$i_{\text{ET}, \text{R}_{\text{ads}}}^{\text{p}} = \frac{F^2vA\Gamma_{\text{R}}}{4RT}$	$I_{\text{ET}, \text{R}_{\text{ads}}}^{\text{p}} = \frac{\theta_{\text{R}}}{4}$

<sup>a</sup> ADMR, ADPR, and AIDPR zones are also included but are not used to define a boundary in Table S-

7. <sup>b</sup> From ref. S-1. <sup>c</sup> From ref. S-2. <sup>d</sup> The maximum value.

**Table S-5. Characteristic Peak and Limiting Currents Controlled by Adsorption Steps**

Adsorbate	Kinetic Zone		Current	
	Case II	Case III	Original	Dimensionless
Saturated	—	AKinDR	$i_{R_{\text{sat}}}^{\text{lim}} = F A k_{\text{des}}^R \Gamma_s$	$I_{R_{\text{sat}}}^{\text{lim}} = \lambda_{\text{des}}^R$
		AIDPR <sup>a</sup>	$i_{R_{\text{sat}}}^{\text{pc}} = \frac{F A k_{\text{ads}}^R c_0 \Gamma_s}{2}$	$I_{R_{\text{sat}}}^{\text{pc}} = \frac{\lambda_{\text{des}}^R \rho_R}{2}$
		AIDPR <sup>b</sup>	$i_{R_{\text{sat}}}^{\text{pa}} = \frac{F A k_{\text{des}}^R \Gamma_s}{2}$	$I_{R_{\text{sat}}}^{\text{pa}} = \frac{\lambda_{\text{des}}^R}{2}$
Unsaturated	KinDR, KinR'	—	$i_{O_{\text{ads}}}^{\text{lim}} = F A k_{\text{des}}^O \Gamma_s \beta_O c_0^c$	$I_{O_{\text{ads}}}^{\text{lim}} = \lambda_{\text{des}}^O \rho_O$
	—	DRAI <sup>c</sup>	$i_{R_{\text{ads}}}^{\text{lim}} = F A k_{\text{ads}}^R \Gamma_s c_0$	$I_{R_{\text{ads}}}^{\text{lim}} = \lambda_{\text{des}}^R \rho_R$
	—	DRKin, DRAI <sup>d</sup>	$i_{R_{\text{ads}}}^{\text{p}} = \frac{F A k_{\text{des}}^R \Gamma_R}{2}$	$I_{R_{\text{ads}}}^{\text{p}} = \frac{\lambda_{\text{des}}^R \theta_R}{2}$

<sup>a</sup> Forward pre-peak. <sup>b</sup> Reverse pre-peak. <sup>c</sup> Not observable (see the text). <sup>d</sup> The maximum value.

**Table S-6. Boundaries between Kinetic Zones in Case II.**

Boundary	Kinetic Zones				Conditions	
	Concerted		Non-Concerted		Currents	Parameters
<b>1</b>	AR	DO	AR	DO	$I_{ET}^p = I_{diff}^p$	$\kappa = 1.7852$
<b>2</b>	DO	KinR	DO	KinR	$I_{diff}^p = I_{ET, O_{ads}}^p$	$\kappa = \frac{1.7852}{\rho_O}$
<b>3</b>	KinR	KinDR	KinR'	KinDR	$I_{ET, O_{ads}}^p = I_{O_{ads}}^{lim}$	$\lambda_{des}^O = \frac{1}{4}$
<b>4</b>	DO	KinDR	DO	KinDR	$I_{diff}^p = I_{O_{ads}}^{lim}$	$\kappa \lambda_{des}^O = \frac{0.4463}{\rho_O}$
<b>5</b>	—	—	AR	KinDR	$I_{ET}^p = I_{O_{ads}}^{lim}$	$\lambda_{des}^O = \frac{1}{4\rho_O}$
<b>6</b>	—	—	KinR	KinR'	$I_{ET, O_{ads}}^p = I_{O_{ads}}^{lim} \times 10$	$\lambda_{des}^O = \frac{1}{4 \times 10}$

**Table S-7. Boundaries between Kinetic Zones in Case III.**

Boundary	Kinetic Zones				Conditions	
	Concerted		Non-Concerted		Currents	Parameters
<b>1</b>	DMR	ADMR	DPR	ADPR	$I_{diff}^p = I_{ET}^p \times 10^2$	$\kappa = 1.7852 \times 10^{-2}$
	—	—	DPR	AIDPR		
<b>2</b>	ADMR	DO	ADPR	DO	$I_{ET}^p = I_{diff}^p$	$\kappa = 1.7852$
	AKinDR	DO	AIDPR	DRKin		
	AR	DO	AIDPR	DRAI		
<b>3</b>	DMR	AKinDR	—	—	$I_{diff}^p = I_{R_{sat}}^{lim}$	$\lambda_{des}^R \kappa = 0.4463$
	ADMR	AKinDR	—	—		
<b>4</b>	AKinDR	AR	—	—	$I_{R_{sat}}^{lim} \times 10 = I_{ET}^p$	$\lambda_{des}^R = \frac{1}{4 \times 10}$
<b>5</b>	—	—	ADPR	AIDPR	$I_{ET}^p = I_{R_{sat}}^{pa}$	$\lambda_{des}^R = \frac{1}{2}$
	—	—	DO	DRKin	$I_{ET, R_{ads}}^p = I_{R_{ads}}^p$	
<b>6</b>	—	—	DRKin <sup>a</sup>	DRAI <sup>b</sup>	$I_{ET, R_{ads}}^p = I_{R_{ads}}^p \times 10^2$	$\lambda_{des}^R = \frac{1}{2 \times 10^2}$
<b>7</b>	—	—	DRAI	DPR	$I_{R_{ads}}^{lim} \times 10 = I_{diff}^p$	$\lambda_{des}^R \kappa = \frac{0.04463}{\rho_R}$
<b>8</b>	—	—	AIDPR	DPR	$I_{R_{ads}}^{pc} = I_{diff}^p$	$\lambda_{des}^R \kappa = \frac{0.8926}{\rho_R}$

<sup>a</sup> The maximum value in Table S-4. <sup>b</sup> The maximum value in Table S-5.

**ET Equivalence.** We obtained equivalences between the rates of ET steps as listed in Table 2. Equivalences between ACET and non-ACET kinetics (entries 1–4 in Table S-8) were obtained by considering the requirement of equilibrium adsorption or chemically irreversible ET. The kinetic equivalences also satisfy the thermodynamic equivalences between concerted and non-concerted mechanisms (Table S-9). Entry 1 or 3 in Table S-8 is possible for Case II or Case III in Table 2, respectively. In Case IV, two ET equivalences with the same requirement are possible, i.e., a combination of entries 1 and 2 or 3 and 4 in Table S-8 for entries 3 or 4 in Table 2, respectively. When both oxidant and reductant maintain equilibrium adsorption in Case IV, all ET steps are equivalent (entry 5 in Table 2). In this case, ET equivalences are expected also between ACET steps as well as between non-ACET steps (entries 5 and 6, respectively, in Table S-8). These equivalences do not result from the chemical irreversibility of the ET steps, which are either reductive or oxidative.

Formal potentials of ACET and non-ACET steps are thermodynamically related to each other (Table S-9) and, subsequently, are not useful for discrimination between concerted and non-concerted mechanisms. The formal potential of an outer-sphere ET step is defined uniquely by the standard chemical potentials of oxidant and reductant in the bulk solution [S-3]. Accordingly, an adsorption step does not contribute to the formal potential of the outer-sphere ET step. By contrast, the formal potential of an ACET step is related to the formal potential of an outer-sphere ET step and the equilibrium constant of the common adsorption step. This relationship is shown by entries 2 and 3 in Table S-9. In Case IV, the formal potentials of inner-sphere and outer-sphere ET steps are thermodynamically related to the equilibrium constants of both adsorption steps (see entry 4). Accordingly, formal potentials are not useful to discriminate between inner-sphere and outer-sphere ET steps in Case IV.



**Table S-8. ET Equivalence and Requirements**

ET Equivalence			Requirement	
ET Rate		Standard ET Rate Constant <sup>a</sup>	Adsorption <sup>b</sup>	ET <sup>c</sup>
$v_C^O = v_{IS}^{O_{ads}}$	$V_C^O = V_{IS}^{O_{ads}}$	$\Lambda_C^O = \Lambda_{IS}^{O_{ads}} (\rho_O)^{1-\alpha}$	$\rho_O C_O = \frac{\theta_O}{\theta_M}$	$V_C^O = -\Lambda_C^O \theta_R (\xi_C^O)^{(1-\alpha)}$ $V_{IS}^{O_{ads}} = -\Lambda_{IS}^{O_{ads}} \theta_R (\xi_{IS}^{O_{ads}})^{(1-\alpha)}$
$v_C^{O_{ads}} = v_{OS}^O$	$V_C^{O_{ads}} = \frac{V_{OS}^O}{\kappa}$	$\Lambda_C^{O_{ads}} = \frac{\Lambda_{OS}^O}{\kappa (\rho_O)^{1-\alpha} \theta_M}$		$V_C^{O_{ads}} = -\Lambda_C^{O_{ads}} C_R \theta_M (\xi_C^{O_{ads}})^{(1-\alpha)}$ $V_{OS}^O = -\Lambda_{OS}^O C_R (\xi_{OS}^O)^{(1-\alpha)}$
$v_C^O = v_{OS}^O$	$V_C^O = \frac{V_{OS}^O}{\kappa}$	$\Lambda_C^O = \frac{\Lambda_{OS}^O}{\kappa \rho_R^\alpha \theta_M}$	$\rho_R C_R = \frac{\theta_R}{\theta_M}$	$V_C^O = \Lambda_C^O C_O \theta_M (\xi_C^O)^{-\alpha}$ $V_{OS}^O = \Lambda_{OS}^O C_O (\xi_{OS}^O)^{-\alpha}$
$v_C^{O_{ads}} = v_{IS}^{O_{ads}}$	$V_C^{O_{ads}} = V_{IS}^{O_{ads}}$	$\Lambda_C^{O_{ads}} = \Lambda_{IS}^{O_{ads}} (\rho_R)^\alpha$		$V_C^{O_{ads}} = \Lambda_C^{O_{ads}} \theta_O (\xi_C^{O_{ads}})^{-\alpha}$ $V_{IS}^{O_{ads}} = \Lambda_{IS}^{O_{ads}} \theta_O (\xi_{IS}^{O_{ads}})^{-\alpha}$
$v_C^O = v_C^{O_{ads}}$	$V_C^O = V_C^{O_{ads}}$	$\Lambda_C^O = \frac{\Lambda_C^{O_{ads}} (\rho_O)^{1-\alpha}}{\rho_R^\alpha}$	$\rho_O C_O = \frac{\theta_O}{\theta_M}$	—
$v_{OS}^O = v_{IS}^{O_{ads}}$	$\frac{V_{OS}^O}{\kappa} = V_{IS}^{O_{ads}}$	$\Lambda_{IS}^{O_{ads}} = \frac{\Lambda_{OS}^O}{\kappa \theta_M (\rho_O)^{1-\alpha} \rho_R^\alpha}$	$\rho_R C_R = \frac{\theta_R}{\theta_M}$	—

<sup>a</sup> See Table S-2 for definitions. <sup>b</sup> Equilibrium. <sup>c</sup> Only reductive or oxidative.

**Table S-9. Thermodynamic Equivalence and Relationships between Formal Potentials**

Thermodynamic Equivalence	Formal Potentials	Case
$\xi_C^O = \frac{\xi_{IS}^{O_{ads}}}{\rho_O}$	$E_C^{O',O} = E_{IS}^{O',O_{ads}} + \frac{RT}{F} \ln \rho_O$	II and IV
$\xi_C^O = \frac{\xi_{OS}^O}{\rho_R}$	$E_C^{O',O} = E_{OS}^{O',O} + \frac{RT}{F} \ln \rho_R$	III and IV
$\xi_C^{O_{ads}} = \rho_O \xi_{OS}^O$	$E_C^{O',O_{ads}} = E_{OS}^{O',O} + \frac{RT}{F} \ln \rho_O$	IV
$\xi_{IS}^{O_{ads}} = \frac{\rho_O}{\rho_R} \xi_{OS}^O$ <sup>a</sup>	$E_{IS}^{O',O_{ads}} + \frac{RT}{F} \ln \rho_O = E_{OS}^{O',O} + \frac{RT}{F} \ln \rho_R$ <sup>a</sup>	

<sup>a</sup> Equivalent to the combination of relationships in entires 1 and 2.

**Quantitative Discrimination between Similar CVs.** In Case II, similar voltammograms with a broad peak before a limiting current during the forward scan are expected for concerted and non-concerted mechanisms around the KinDR zone. The respective CVs are shown in Figure S-1A and S-1B but can be discriminated from each other because the corresponding adsorption parameters are different. Specifically, CVs with similar shapes are expected for both mechanisms at the boundary between KinDR and DO zones (Figure S-1A). The normalised current is  $2.5 \times 10^3$  times higher for the non-concerted mechanism. This difference corresponds to a  $2.5 \times 10^3$  times lower concentration of adsorption sites when the scan rate and the electrode area are identical. By contrast, the  $\kappa$  value is  $2.0 \times 10^4$  times lower for the non-concerted mechanism. This difference corresponds to a  $2.0 \times 10^4$  times lower concentration of adsorption sites for the same scan rate and oxidant concentration as the concerted mechanism in eq 17. Accordingly, the similarly shaped CVs are distinguishable by quantitatively evaluating the current. Moreover, similar CVs around the boundary of the KinDR zone with KinR and

AR zones are expected for concerted and non-concerted mechanisms, respectively, but are distinguishable quantitatively (Figure S-1B). In this case, the normalised current is  $1.05 \times 10^4$  times higher for the non-concerted mechanism. The  $\kappa$  value, however, is  $2.0 \times 10^8$  times lower for the non-concerted mechanism.

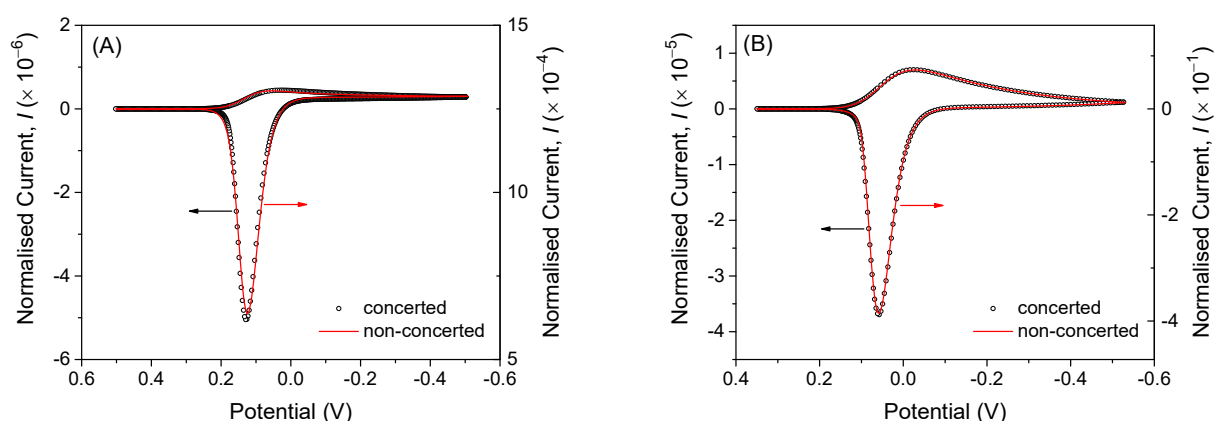


**Figure S-1.** CVs based on concerted and non-concerted mechanisms with  $\rho_0 = 1 \times 10^{-4}$  in addition to (A)  $\lambda_{\text{des}}^{\text{O}} = 2.5 \times 10^{-3}$  and  $\kappa = 1.79 \times 10^6$  and  $\lambda_{\text{des}}^{\text{O}} = 1.25 \times 10$  and  $\kappa = 8.9 \times 10$ , respectively, and (B)  $\lambda_{\text{des}}^{\text{O}} = 1.0 \times 10^{-1}$  and  $\kappa = 1.0 \times 10^6$  and  $\lambda_{\text{des}}^{\text{O}} = 1.0 \times 10^3$  and  $\kappa = 1.0 \times 10^{-2}$ , respectively. The normalised current is defined by eq 9. The potential is defined against  $E_{\text{OS}}^{\text{O},\text{O}}$ . Parameters for parts (A) and (B) are indicated by closed and open circles in Figures 1A and 1B, respectively.

**Adsorption-Coupled Reduction of Benzyl Chloride.** We simulated dimensionless CVs for the adsorption-coupled reduction of benzyl chloride reduction at the silver electrode by employing concerted and non-concerted mechanisms (Figure 4). Diffusion equations are defined by eqs 10 and S-1

for species A and B. The homogeneous chemical reactions of species C and D are irreversible and considered in the diffusion equations as given by

$$\frac{\partial c_C}{\partial t} = D \left( \frac{\partial^2 c_C}{\partial x^2} \right) - k_{\text{prot}}^C c_C \quad (\text{S-18})$$

$$\frac{\partial c_D}{\partial t} = D \left( \frac{\partial^2 c_D}{\partial x^2} \right) + k_{\text{prot}}^C c_C \quad (\text{S-19})$$

where  $k_{\text{prot}}^C$  is the protonation rate constant. The corresponding dimensionless equations are given by

$$\frac{\partial C_C}{\partial \tau} = \left( \frac{\partial^2 C_C}{\partial X^2} \right) - K_{\text{prot}}^C C_C \quad (\text{S-20})$$

$$\frac{\partial C_D}{\partial \tau} = \left( \frac{\partial^2 C_D}{\partial X^2} \right) + K_{\text{prot}}^C C_C \quad (\text{S-21})$$

with

$$K_{\text{prot}}^C = \frac{k_{\text{prot}}^C RT}{F\nu} \quad (\text{S-22})$$

In addition, an irreversible chemical reaction is defined for adsorbed forms of species C and D to yield a reaction rate as

$$\nu_{\text{prot}}^C \text{ads} = k_{\text{prot}}^C \text{ads} \Gamma_C \quad (\text{S-23})$$

where  $k_{\text{prot}}^C \text{ads}$  is the protonation rate constant. The dimensionless reaction rate is given by

$$V_{\text{prot}}^C \text{ads} = \nu_{\text{prot}}^C \text{ads} \frac{RT}{\Gamma_C F\nu} = K_{\text{prot}}^C \text{ads} \theta_C \quad (\text{S-24})$$

with

$$K_{\text{prot}}^C \text{ads} = \frac{k_{\text{prot}}^C \text{ads} RT}{F\nu} \quad (\text{S-25})$$

The current response was based only on ET steps and obtained for the concerted mechanism by

$$i = v_C^A + v_C^B + v_C^{A_{\text{ads}}} + v_C^{B_{\text{ads}}} \quad (\text{S-26})$$

and for the non-concerted mechanism by

$$i_{\text{et}} = v_{\text{OS}}^A + v_{\text{OS}}^B + v_{\text{IS}}^{A_{\text{ads}}} + v_{\text{IS}}^{B_{\text{ads}}} \quad (\text{S-27})$$

The normalised current response was obtained by using eq 9 as

$$I = V_C^A + V_C^B + V_C^{A_{\text{ads}}} + V_C^{B_{\text{ads}}} \quad (\text{S-28})$$

for the concerted mechanism and

$$I = \frac{V_{\text{OS}}^A + V_{\text{OS}}^B}{\kappa} + V_{\text{IS}}^{A_{\text{ads}}} + V_{\text{IS}}^{B_{\text{ads}}} \quad (\text{S-29})$$

for the non-concerted mechanism. The normalised current based on each ET step is plotted in Figures 5B, 5C, 5E, and 5F. In both mechanisms, experimental conditions and concentration of adsorption sites are common (Table S-10), thereby yielding the same  $\kappa$  value from eq 17.

**Table S-10. Common Parameters for the Adsorption-Coupled Reduction of Benzyl Chloride<sup>a</sup>**

$v$ [V/s]	$D$ [cm <sup>2</sup> /s]	$c_0$ [mM]	$\Gamma_s$ (mol/cm <sup>2</sup> )	$\kappa$
500	$1.03 \times 10^{-5}$	5	$6.64 \times 10^{-10}$	5.8

<sup>a</sup> Parameters were obtained from ref. S-4.

The diffusion equations were solved by considering the boundary conditions summarised in Table S-11. Reaction parameters were obtained by fitting the major wave of experimental CVs with the non-concerted mechanism [S-4] and used in this work. Specifically, parameters of inner-sphere and outer-sphere ET steps in the non-concerted mechanism were converted to those of ACET steps (see Table S-8) as listed in Table S-12. Parameters for adsorption and chemical reaction steps are common for both mechanisms as listed in Table S-13, where the surface concentration of the adsorption site is

$\Gamma_M = \Gamma_s - \Gamma_A - \Gamma_B - \Gamma_C - \Gamma_D$ . Simulated CVs are shown in Figures 5A–5C and the corresponding concentrations of major species, A, D, A<sub>ads</sub>, and C<sub>ads</sub>, are shown in Figure S-2. In addition, CVs were simulated without the irreversible chemical steps (Figures 5D–5F). In Figures 5B, C, E, and F, only the first or second ET step was considered to simulate the normalised current based on eqs S-28 and S-29.

**Table S-11. Electrode Surface Boundary Conditions for Non-Concerted and Concerted Reduction of Benzyl Chloride**

	Non-Concerted Mechanism		Concerted Mechanism	
Species	Original Condition	Dimensionless Condition	Original Condition	Dimensionless Condition
A	$-D \left( \frac{\partial c_A}{\partial x} \right) = -v_{OS}^A - v_{ads}^A$	$-\left( \frac{\partial C_A}{\partial X} \right) = -V_{OS}^A - \kappa V_{ads}^A$	$-D \left( \frac{\partial c_A}{\partial x} \right) = -v_C^A - v_{ads}^A$	$-\left( \frac{\partial C_A}{\partial X} \right) = -\kappa (V_C^A + V_{ads}^A)$
A <sub>ads</sub>	$\left( \frac{\partial \Gamma_A}{\partial t} \right) = -v_{IS}^A + v_{ads}^A$	$\left( \frac{\partial \theta_A}{\partial \tau} \right) = -V_{IS}^A + V_{ads}^A$	$\left( \frac{\partial \Gamma_A}{\partial t} \right) = -v_C^A + v_{ads}^A$	$\left( \frac{\partial \theta_A}{\partial \tau} \right) = -V_C^A + V_{ads}^A$
B	$-D \left( \frac{\partial c_B}{\partial x} \right) = v_{OS}^A - v_{OS}^B - v_{ads}^B$	$-\left( \frac{\partial C_B}{\partial X} \right) = V_{OS}^A - V_{OS}^B - \kappa V_{ads}^B$	$-D \left( \frac{\partial c_B}{\partial x} \right) = v_C^A - v_C^B - v_{ads}^B$	$-\left( \frac{\partial C_B}{\partial X} \right) = \kappa (V_C^A - V_C^B - V_{ads}^B)$
B <sub>ads</sub>	$\left( \frac{\partial \Gamma_B}{\partial t} \right) = v_{IS}^A - v_{IS}^B + v_{ads}^B$	$\left( \frac{\partial \theta_B}{\partial \tau} \right) = V_{IS}^A - V_{IS}^B + V_{ads}^B$	$\left( \frac{\partial \Gamma_B}{\partial t} \right) = v_C^A - v_C^B + v_{ads}^B$	$\left( \frac{\partial \theta_B}{\partial \tau} \right) = V_C^A - V_C^B + V_{ads}^B$
C	$-D \left( \frac{\partial c_C}{\partial x} \right) = v_{OS}^B - v_{ads}^C$	$-\left( \frac{\partial C_C}{\partial X} \right) = V_{OS}^B - \kappa V_{ads}^C$	$-D \left( \frac{\partial c_C}{\partial x} \right) = v_C^B - v_{ads}^C$	$-\left( \frac{\partial C_C}{\partial X} \right) = \kappa (V_C^B - V_{ads}^C)$
C <sub>ads</sub>	$\left( \frac{\partial \Gamma_C}{\partial t} \right) = v_{IS}^B + v_{ads}^C - v_{prot}^C$	$\left( \frac{\partial \theta_C}{\partial \tau} \right) = V_{IS}^B + V_{ads}^C - V_{prot}^C$	$\left( \frac{\partial \Gamma_C}{\partial t} \right) = v_C^B + v_{ads}^C - v_{prot}^C$	$\left( \frac{\partial \theta_C}{\partial \tau} \right) = V_C^B + V_{ads}^C - V_{prot}^C$
D	$-D \left( \frac{\partial c_D}{\partial x} \right) = -v_{ads}^D$	$-\left( \frac{\partial C_D}{\partial X} \right) = -\kappa V_{ads}^D$	$-D \left( \frac{\partial c_D}{\partial x} \right) = -v_{ads}^D$	$-\left( \frac{\partial C_D}{\partial X} \right) = -\kappa V_{ads}^D$
D <sub>ads</sub>	$\left( \frac{\partial \Gamma_D}{\partial t} \right) = v_{prot}^C + v_{ads}^D$	$\left( \frac{\partial \theta_D}{\partial \tau} \right) = V_{prot}^C + V_{ads}^D$	$\left( \frac{\partial \Gamma_D}{\partial t} \right) = v_{prot}^C + v_{ads}^D$	$\left( \frac{\partial \theta_D}{\partial \tau} \right) = V_{prot}^C + V_{ads}^D$

**Table S-12. ET Parameters for Non-Concerted and Concerted Reduction of Benzyl Chloride**

Non-Concerted Mechanism <sup>a</sup>					Concerted Mechanism <sup>b</sup>	
ET Reaction	$E_{OS}^{0,i}$ [V] <sup>c</sup>	$\alpha$	$k_{OS}^{0,i}$ [cm/s] <sup>c</sup>	$\Lambda_{OS}^{i,c}$	ET Reaction	$\Lambda_C^{i,c}$
A + e $\rightleftharpoons$ B	-0.8	0.28	$3.58 \times 10^{-10}$	$8.00 \times 10^{-10}$	A + e $\rightleftharpoons$ B <sub>ads</sub>	$3.41 \times 10^{-11}$
B + e $\rightleftharpoons$ C	-1.45	0.50	1	2.23	B + e $\rightleftharpoons$ C <sub>ads</sub>	$5.34 \times 10^{-10}$
	$E_{IS}^{0,i_{ads}}$ [V] <sup>c</sup>	$\alpha$	$k_{IS}^{0,i_{ads}}$ [1/s] <sup>c</sup>	$\Lambda_{IS}^{i_{ads}c}$		$\Lambda_C^{i_{ads}c}$
A <sub>ads</sub> + e $\rightleftharpoons$ B <sub>ads</sub>	-0.626	0.42	$1.1 \times 10^{-6}$	$5.65 \times 10^{-11}$	A <sub>ads</sub> + e $\rightleftharpoons$ B	$3.44 \times 10^{-6}$
B <sub>ads</sub> + e $\rightleftharpoons$ C <sub>ads</sub>	-1.01	0.5	10	$5.14 \times 10^{-4}$	B <sub>ads</sub> + e $\rightleftharpoons$ C	$5.75 \times 10^1$

<sup>a</sup> Parameters were obtained from ref. S-4. <sup>b</sup> Parameters were calculated from those of the non-concerted mechanism as listed in Table S-8 except for  $\Lambda_C^A$ , which was adjusted to obtain a good fit between concerted and non-concerted mechanisms (see Figure 5A). <sup>c</sup> i = A or B.



**Table S-13. Adsorption and Chemical Reaction Parameters for Reduction of Benzyl Chloride**

Reaction	Original Parameter <sup>a</sup>		Dimensionless Parameter	
A $\rightleftharpoons$ A <sub>ads</sub>	$k_{\text{ads}}^{\text{A}}$ [1/M/s]	$4.3 \times 10^4$	$\lambda_{\text{des}}^{\text{A}}$	$4.70 \times 10^{-2}$
	$\beta_{\text{A}}$ [1/M]	$4.7 \times 10^1$	$\rho_{\text{A}}$	$2.35 \times 10^{-1}$
B $\rightleftharpoons$ B <sub>ads</sub>	$k_{\text{ads}}^{\text{B}}$ [1/M/s]	$1.0 \times 10^2$	$\lambda_{\text{des}}^{\text{B}}$	$1.22 \times 10^{-7}$
	$\beta_{\text{B}}$ [1/M]	$4.2 \times 10^4$	$\rho_{\text{B}}$	$2.10 \times 10^2$
C $\rightleftharpoons$ C <sub>ads</sub>	$k_{\text{ads}}^{\text{C}}$ [1/M/s]	$1.0 \times 10^2$	$\lambda_{\text{des}}^{\text{C}}$	$2.06 \times 10^{-15}$
	$\beta_{\text{C}}$ [1/M]	$2.5 \times 10^{12}$	$\rho_{\text{C}}$	$1.25 \times 10^{10}$
D $\rightleftharpoons$ D <sub>ads</sub>	$k_{\text{ads}}^{\text{D}}$ [1/M/s]	$1.0 \times 10^2$	$\lambda_{\text{des}}^{\text{D}}$	$5.14 \times 10^3$
	$\beta_{\text{D}}$ [1/M]	$1.0 \times 10^{-6}$	$\rho_{\text{D}}$	$5.0 \times 10^{-9}$
C $\rightarrow$ D	$k^{\text{prot}}$ [1/s]	$1.0 \times 10^{10}$	$K^{\text{prot}}$	$5.14 \times 10^5$
C <sub>ads</sub> $\rightarrow$ D <sub>ads</sub>	$k_{\text{ads}}^{\text{prot}}$ [1/s]	$1.5 \times 10^3$	$K_{\text{ads}}^{\text{prot}}$	$7.71 \times 10^{-2}$

<sup>a</sup> Parameters were obtained from ref. S-4.

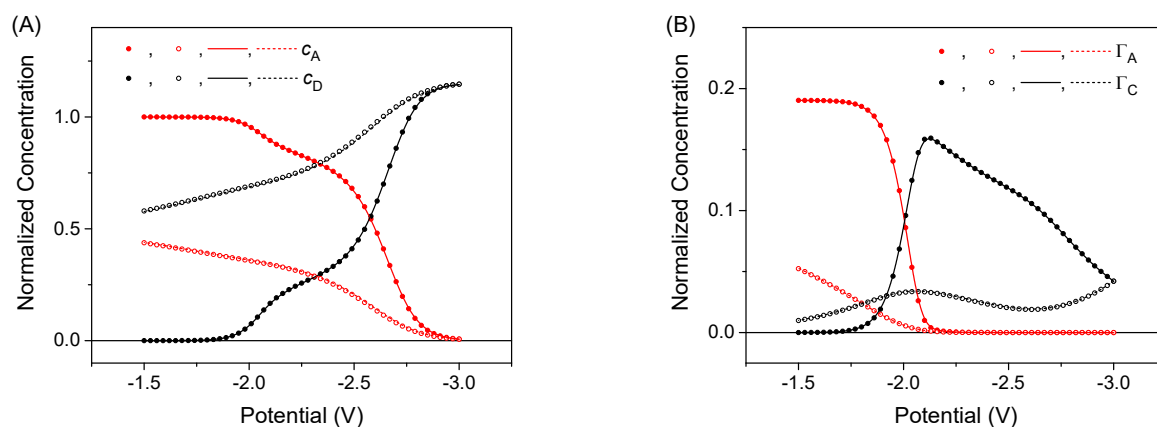


**Figure S-2.** Concentrations of major species (A) near and (B) on the electrode surface in concerted (circles) and non-concerted (lines) mechanisms. Closed circles and solid lines represent the forward scan. Open circles and dotted lines represent the reverse scan.

## REFERENCES

- [S-1] A.J. Bard, L.R. Faulkner, H.S. White, *Electrochemical Methods: Fundamentals and Applications*, 3rd ed., John Wiley & Sons, New York, 2022, p. 316.
- [S-2] Ref. S-1, p. 759.
- [S-3] Ref. S-1, p. 87.
- [S-4] O.V. Klymenko, O. Buriez, E. Labbe, D.P. Zhan, S. Rondinini, Z.Q. Tian, I. Svir, C. Amatore, Uncovering the missing link between molecular electrochemistry and electrocatalysis: Mechanism of the reduction of benzyl chloride at silver cathodes, *ChemElectroChem*, 1 (2014) 227–240.